Trop J Nat Prod Res, April 2026; 10(4): 8741 - 8747 **ISSN 2616-0684 (Print)**
ISSN 2616-0692 (Electronic)

Tropical Journal of Natural Product Research

Available online at https://www.tjnpr.org

Original Research Article

Potent α-Glucosidase Inhibition by a Non-Psychoactive CBG/CBD-Rich Cannabis Extract

Chutima Kaewpiboon[1], Abdul-Wahab Salae[2] and Nawong Boonnak[3]*

[1]*Program in Biotechnology, Faculty of Science and Digital Innovation, Thaksin University, Phatthalung, 93210, Thailand*
[2]*Program in Science, Faculty of Science and Technology, Phuket Rajabhat University, Phuket 83000, Thailand*
[3]*Education Program in Science and Technology, Faculty of Science and Digital Innovation, Thaksin University, Phatthalung 93210, Thailand*

ARTICLE INFO

Article history:
Received 01 March 2026
Revised 28 March 2026
Accepted 06 April 2026
Published online 01 May 2026

ABSTRACT

Cannabinoids from *Cannabis sativa* have attracted increasing attention as potential adjuncts for diabetes management due to their ability to inhibit carbohydrate-digesting enzymes. This study aimed to investigate the α-glucosidase inhibitory activity of purified cannabinoids and chemotyped cannabis extracts to identify potent non-psychoactive candidates. Purified delta-9-tetrahydrocannabinol (THC), cannabidiol (CBD), and cannabinol (CBN) were first evaluated in vitro. Among these compounds, THC exhibited the strongest inhibitory activity (IC_{50} = 90.19±3.14 µg/mL), followed by CBD (IC_{50} = 331.54±7.45 µg/mL) and CBN (IC_{50} = 536.65 ± 9.85 µg/mL). For comparison, the reference drug acarbose showed an IC_{50} value of (484.10± 4.26 µg/mL) under the same assay conditions. Because the psychoactive nature and regulatory restrictions of THC limit its direct application, several cannabis chemotype extracts with distinct cannabinoid profiles were subsequently examined. Among the crude extracts, the THC-rich chemotype (Black Dragon) showed the strongest inhibition (IC_{50} = 271.77 ± 6.98 µg/mL). Notably, a hybrid chemotype designated CBG-F1, characterized by a balanced CBG:CBD ratio of approximately 1:1.3, demonstrated markedly stronger activity (IC_{50} = 111.51±8.42 µg/mL), approaching the potency of purified THC despite containing no major psychoactive cannabinoids. Enzyme kinetic analysis using Lineweaver–Burk plots revealed that CBG-F1 acts as a non-competitive inhibitor of α-glucosidase, reducing catalytic activity without affecting substrate binding affinity. These findings highlight the potential of CBG/CBD-rich cannabis chemotypes as promising non-psychoactive sources of α-glucosidase inhibitors and support their further development as functional ingredients for supportive antidiabetic applications.

Keywords: Cannabinoids, Antidiabetic potential, *Cannabis* sp. Chemotype, Cannabigerol (CBG), Cannabidiol (CBD)

Introduction

Cannabis sativa L. is considered one of the oldest cultivated plants, with evidence of human use as a source of fiber, and oil, as well as for medicinal purposes.[1] The main active compound as cannabinoids identified in this species—including cannabigerol (CBG, Δ-9-tetrahydrocannabinol (THC), cannabinol (CBN), cannabichromene (CBC) and cannabidiol (CBD)—constitute a bioactive compounds that interact with the human endocannabinoid system. Each of these cannabinoids exhibits distinct pharmacological effects, ranging from psychoactive and analgesic actions to anti-inflammatory and neuroprotective properties, which has led to growing scientific and medical interest in their potential applications.[2] *C. sativa* L. is often separated into multiple subspecies and varieties. Each group displays a characteristic pattern of major cannabinoids, distinguished mainly by differences in their relative abundances

*Corresponding author. Email: nawong@tsu.ac.th
Tel: +66945950495

Citation: Kaewpiboon C, Salae AW, Boonnak N. Potent α-glucosidase inhibition by a non-psychoactive CBG/CBD rich cannabis extract. Trop J Nat Prod Res. 2026; 10(4): 8741 – 8747 https://doi.org/10.26538/tjnpr/v10i4.58

Official Journal of Natural Product Research Group, Faculty of Pharmacy, University of Benin, Benin City, Nigeria

In medical and pharmacological contexts, a chemotaxonomic scheme is frequently used to classify plants into five chemotypes (chemical phenotypes) according to their predominant cannabinoid content. Drug-type plants are designated chemotype I with a markedly elevated THC/CBD ratio (>1.0), whereas those with an intermediate THC/CBD ratio (approximately 0.5–2.0) are described as chemotype II. A fibre-type plants with a low THC/CBD ratio (<1.0) are assigned to chemotype III, while chemotype IV comprises fibre-type plants in which CBG is the principal cannabinoid. Chemotype V encompasses fibre-type *Cannabis* that contains only trace or undetectable levels of cannabinoids.[3] Preparations obtained from different plant chemotypes may exhibit markedly different biological activities, including variable antidiabetic potential, depending on the composition and synergistic interactions of cannabinoids capable of inhibiting α-glucosidase. As a result, α-glucosidase inhibitors have attracted attention as a non-invasive therapeutic approach, generally associated with mild, transient, and dose-dependent gastrointestinal side effects, including diarrhea, abdominal discomfort and flatulence.[4] By delaying intestinal carbohydrate digestion and absorption, these inhibitors effectively attenuate postprandial blood glucose excursions.[5] In recent decades, natural products have attracted increasing attention as potential therapeutic agents with enhanced efficacy and improved therapeutic profiles, particularly for the prevention and treatment of type 2 diabetes via α-glucosidase inhibitory activity.[6]

Among the major cannabinoids, THC and CBD have been most extensively investigated, with in vitro studies demonstrating that both compounds inhibit α-glucosidase. However, THC exhibits greater potency than CBD.[7] A key dilemma is that THC, one of the most potent cannabinoid α-glucosidase inhibitors reported to date, is psychoactive and classified as a controlled substance in many jurisdictions,[8] creating legal and safety barriers to its use as an antidiabetic ingredient. While

ISSN 2616-0684 (Print)
ISSN 2616-0692 (Electronic)

structurally related cannabinoids such as cannabinol (CBN) may pose somewhat fewer concerns regarding psychoactivity, their inhibitory activities appear weaker than those of THC.[9] Conversely, non-psychoactive cannabinoids such as CBD and CBG offer clear regulatory and safety advantages. CBN, a non-enzymatic oxidative metabolite of THC, and 8-hydroxycannabinol (8-OH-CBN) have also been shown to exert notable rat intestinal α-glucosidase inhibition. They were the most potent inhibitors retarding the enzymes through a noncompetitive mechanism.[10] In contrast, cannabichromene (CBC) has typically displayed weaker α-glucosidase inhibition relative to THC and CBN, indicating that structural differences within the cannabinoid scaffold strongly influence enzyme binding and inhibitory potency.[10] Evidence for cannabigerol (CBG), the biosynthetic precursor of several major cannabinoids, remains more limited; however, emerging data point to a broader antidiabetic potential of CBG through modulation of metabolic and inflammatory pathways, raising the possibility that CBG may also contribute to α-glucosidase inhibition either directly or in combination with other cannabinoids.[11] The selection of the hybrid chemotypes was not arbitrary but grounded in both biochemical and pharmacological considerations. Previous studies have demonstrated that individual cannabinoids such as CBD exhibit moderate inhibitory activity against α-glucosidase, although with relatively limited potency.[12] In contrast, several reports have shown that full-spectrum cannabis extracts display enhanced biological activity compared to isolated cannabinoids, likely due to synergistic interactions among multiple constituents.[13,14,15] These findings suggest that combinatorial interactions between cannabinoids may play a critical role in enhancing α-glucosidase inhibitory effects.

To address these questions, the present study systematically evaluated the α-glucosidase inhibitory activity of purified cannabinoids, including THC, CBN, and CBD, as well as a panel of *C. sativa* chemotype extracts with varying proportions of THC, CBD, and CBG. The tested chemotypes included a THC-rich strain, Black Dragon, characterized by high THC content with low levels of CBD and CBG; a CBG-rich strain, SUT11, developed from fiber-type lineage and containing predominantly CBG with negligible THC; and a CBD-rich strain, BLC-1C, representing a non-psychoactive chemotype high in CBD. In addition, two hybrid strains—CBD-purple (CBD/THC hybrid, CBD/THC = 1:1.2) and CBG-F1, which displays a combined predominance of CBG and CBD (CBG/CBD = 1:1.3) with minimal psychoactive cannabinoids—were included to explore the impact of mixed cannabinoid profiles on enzyme inhibition. Particular emphasis was placed on comparing the THC-rich chemotype Black Dragon with the non-psychoactive CBG/CBD-rich hybrid CBG-F1 in order to identify a candidate extract that combines high inhibitory potency with the absence of controlled psychotropic cannabinoids, and to characterize its mode of inhibition using enzyme kinetic analysis.

Materials and Methods

Extraction and Isolation

Dried cannabis inflorescences (500 g) were finely ground and extracted with ethanol (3 × 1.0 L) at room temperature using an ultrasonic bath. The combined extracts were filtered and concentrated under reduced pressure using a rotary evaporator to afford a dark green, viscous ethanolic crude extract (22.34 g), corresponding to 4.46% of the dry flower weight. In Scheme 1 for chemical fractionation, a portion of the ethanolic crude extract (20.00 g) was subjected to vacuum liquid chromatography (VLC). The separation was performed on a column (inner diameter 12.0 cm) packed with silica gel 60H (Merck, 5–40 µm; 0.94 kg), with a sample layer height of 0.8 cm and a silica bed height of 8.0 cm. Elution was carried out using a polarity-gradient solvent system from 100% n-hexane to 100% methanol, collecting 500 mL per fraction. Solvents were removed from each fraction under reduced pressure, and the eluates were monitored by thin-layer chromatography (TLC). Fractions exhibiting similar TLC profiles were combined to yield eight pooled fractions, designated CF1–CF8. Fraction CF-2, obtained as an orange, viscous material (2.874 g), was further separated by VLC. The separation was performed on a column with an inner diameter of 6.00 cm, a sample layer height of 0.50 cm, and a packed bed height of 5.00 cm, using 141.3 g of silica gel.

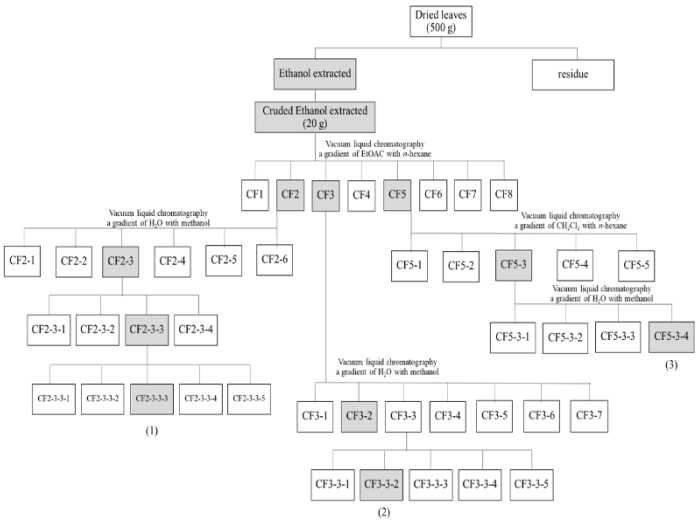

Scheme 1: Schematic overview of the extraction of the ethanolic extract from dried Cannabis sativa inflorescences (500 g), showing successive vacuum liquid chromatography steps on normal-phase and C18 reversed-phase silica to generate fractions CF1–CF8 and their subfractions (CF2-n, CF3-n, CF5-n), and highlighting the active fractions that yielded the purified cannabinoids Δ-9-tetrahydrocannabinol (1; THC,), cannabinol (2; CBN), and cannabidiol (3; CBD)

The column was wet-packed with C18-reversed phase silica gel (Merck, 15–25 µm) and eluted with a stepwise polarity gradient from 50% water/methanol to 100% methanol. Eluates were collected in 100 mL fractions and concentrated under reduced pressure using a rotary evaporator. The resulting fractions were monitored by TLC, and those showing similar TLC profiles were combined to afford six subfractions, designated CF2-1 to CF2-6. Fraction CF2-3, obtained as a yellow, viscous material (0.878 g), was further purified by VLC. The separation was carried out on a column with an inner diameter of 3.00 cm, a sample layer height of 0.50 cm, and a packed bed height of 4.00 cm, using 28.26 g of silica gel. The column was packed with C18-reversed phase silica gel (Merck, 15–25 µm) and eluted with a gradient of 30% water/methanol to 100% methanol. Eluates were collected in 25 mL fractions and concentrated under reduced pressure using a rotary evaporator. The fractions were monitored by TLC, and those displaying similar TLC profiles were combined to yield four subfractions, designated CF2-3-1 to CF2-3-4. Fraction CS2-3-3, obtained as a pale yellow, viscous material (0.372 g), was further purified by VLC. The separation was performed on a column with an inner diameter of 2.00 cm, a sample layer height of 0.50 cm, and a packed bed height of 5.00 cm, using 15.70 g of silica gel. The column was packed with C18-reversed phase silica gel (Merck, 15–25 µm) and eluted with a polarity-gradient system from 40% water/methanol to 100% methanol. Eluates were collected in 10 mL fractions and concentrated under reduced pressure using a rotary evaporator. The fractions were monitored by TLC, and those exhibiting similar TLC profiles were combined to afford five subfractions, designated CF2-3-3-1 to CF2-3-3-5. Fraction CF2-3-3-3 was obtained as a pure compound and designated as Δ-9-tetrahydrocannabinol (THC) (**1**, 76 mg). Fraction CF3-2, obtained as a yellow, viscous material (0.175 g), was further purified by VLC. The separation was carried out on a column with an inner diameter of 1.50 cm, a sample layer height of 0.3 cm, and a packed bed height of 4.00 cm, using 7.06 g of silica gel. The column was packed with C18-reversed-phase silica gel (Merck, 15–25 µm) and eluted with a gradient from 10% water/methanol to 100% methanol. Eluates were collected in 5 mL fractions and concentrated under reduced pressure using a rotary evaporator. Fractions exhibiting similar TLC profiles were combined to give three subfractions, designated CF3-2-1 to CF3-2-3. Fraction CF3-2-2 was obtained as a pure compound and designated as cannabinol (CBN) (**2**, 83 mg). Fraction CF5-3, obtained

as a yellow, viscous material (0.973 g), was further purified by VLC. The separation was carried out on a column with an inner diameter of 3.50 cm, a sample layer height of 0.45 cm, and a packed bed height of 4.00 cm, using 38.46 g of silica gel. The column was packed with C18-reversed-phase silica gel (Merck, 15–25 µm) and eluted with a gradient from 20% water/methanol to 100% methanol. Eluates were collected in 25 mL fractions and concentrated under reduced pressure using a rotary evaporator. Fractions exhibiting similar thin-layer chromatography (TLC) profiles were combined to afford five subfractions, designated CF5-3-1 to CF5-3-5. Fraction CF5-3-4 was obtained as a pure compound and designated as cannabidiol (CBD) (**3**, 185 mg).

Plant materials

Inflorescences of *C. sativa* were obtained from certified seeds of the five chemotypes that were purchased from a commercial seed bank and cultivated under controlled greenhouse conditions in Songkhla Province, Thailand. At the full flowering stage, inflorescences of *C. sativa* were harvested from the following chemotypes: THC-rich (Black Dragon), CBD-rich (BLC-1C), hybrid THC/CBD (CBD-purple), CBG-rich (SUT11), and CBG/CBD (1:1.3; CBG-F1). Briefly, the dried powders (2 g) were soaked in ethanol (20 ml) for 10 days. After that, the extracts were filtrated through a filter paper and subjected to solvent evaporation using a rotary evaporator at 50 °C to yield *C. sativa* inflorescence extracts. The dried extracts were subjected to quantitative HPLC determination of cannabinoid content.

Preparation of cannabis extraction

The dried powders of inflorescences of the following chemotypes were separately extracted using a maceration: THC-rich (Black dragon), CBD-rich (BLC-1C), hybrid THC/CBD (CBD-purple), CBG-rich (SUT11), and CBG/CBD (1:1.3; CBG-F1). Briefly, the dried powders (2 g) were soaked in ethanol (20 ml) for 10 days. After that, the extracts were filtrated through a filter paper and subjected to solvent evaporation using a rotary evaporator at 50 °C to yield *C. sativa* inflorescence extracts. The dried extracts were subjected to quantitative HPLC determination of cannabinoid content.

Quantitative HPLC determination of Cannabinoids

The mobile phase consisted of 0.1% formic acid in deionized (DI) water (solvent A) and 0.1% formic acid in acetonitrile (solvent B). Solvent A was prepared by diluting 1 mL of formic acid to 1,000 mL with DI water, and solvent B by diluting 1 mL of formic acid to 1,000 mL with HPLC-grade acetonitrile. Both solvents were filtered through a 0.45 µm membrane filter and degassed in an ultrasonic bath for 30 min before use. Chromatographic conditions were optimized by varying the mobile phase composition and flow rate of the and by assessing their influence on the separation of a 10 µg/mL mixed cannabinoid standard solution Injections were performed on a C18 column (5 µm, 150 × 4.6 mm), using isocratic mobile-phase ratios of solvent A:solvent B ranging from 20:80 to 60:40 (v/v). UV detection was carried out at 220 nm. For sample preparation, each cannabis extract was dissolved to a final concentration of 1 mg/mL, then filtered through a 0.45 µm membrane filter. The filtrate was transferred to sealed autosampler vials and subsequently analyzed by HPLC under the optimized conditions.

α-Glucosidase inhibition assay

α-Glucosidase inhibitory activity was determined. Briefly, α-glucosidase enzyme (0.1 Unit/ml) was dissolved in 0.1 M phosphate buffer (pH 6.8). The samples were dissolved in DMSO (final DMSO concentration did not exceed 7%). Subsequently, 20 µl of each sample was added with 20 µl of enzyme solution in a 96-well microtiter plate, then incubated at 37 °C for 10 min. After that, pNPG (40 µl) was mixed, and the mixture was further incubated at 37 °C for 40 min. After incubation, 0.2 mM Na_2CO_3 in phosphate buffer (80 µl) was added to each well to stop the reaction. The amount of *p*-nitrophenol was measured using a microplate reader at 405 nm. The blank control was performed by using the same protocol, but the α-glucosidase enzyme solution was replaced with the buffer solution. The control experiment also performed with the same process, but the sample solution was replaced with the same concentration of DMSO and deionized water in the sample solution. Acarbose was used as a positive control. The experiments were carried out in triplicate.

The percentage inhibition was calculated using the following equation:

$$\%\text{Inhibition} = [(\text{Ac-Ab}) - (\text{As-Ab})] / (\text{Ac-Ab}) \times 100$$

Where: Ac = Absorbance of control, As = Absorbance of sample, Ab = Absorbance of blank.

Kinetic Study of α-Glucosidase Inhibition

The inhibition pattern of yeast α-glucosidase was evaluated using *p*-nitrophenyl-α-D-glucopyranoside (pNPG) as the substrate. The test extracts/compounds were prepared at final concentrations of 31.25, 62.5, and 125 µg/mL. An aliquot of each test sample (10 µL) was mixed with 30 µL of phosphate buffer (pH 6.9) and 20 µL of α-glucosidase solution in a 96-well microplate, followed by pre-incubation at 37 °C for 10 min. The reaction was initiated by adding 40 µL of pNPG solution at varying concentrations, and the mixture was further incubated at 37 °C for a defined period. The release of *p*-nitrophenol was monitored spectrophotometrically at 405 nm using a microplate reader, and all measurements were performed in triplicate with acarbose as the positive control. The inhibition type was determined using Lineweaver–Burk plots, constructed from the reciprocal of initial reaction velocities versus the reciprocal of pNPG concentrations in the presence of different inhibitor concentrations. Secondary plots of the slopes and/or intercepts of the Lineweaver–Burk plots against inhibitor concentration were used to calculate the inhibition constants (Ki), thereby elucidating the underlying inhibition mechanism.

Statical analysis

The results are expressed as mean ± SD. Statistical significance was calculated using one-way analysis of variance (ANOVA) followed by Tukey's multiple range test ($p < 0.05$).

Results and Discussion

Extraction and Isolation

To identify the bioactive constituents responsible for α-glucosidase inhibition, an activity-guided fractionation strategy was applied to the ethanolic inflorescence extract. In cannabis trichomes, the key phytocannabinoids arise biosynthetically from the condensation of olivetolic acid and geranyl pyrophosphate to form cannabigerolic acid (CBGA), which serves as the central precursor that is enzymatically cyclized to Δ⁹-tetrahydrocannabinolic acid (THCA) and cannabidiolic acid (CBDA), and subsequently decarboxylated by heat to yield Δ⁹-tetrahydrocannabinol (THC) and cannabidiol (CBD), while oxidative conversion of Δ⁹-THC affords cannabinol (CBN) (**Figure 1**). Reflecting this biosynthetic relationship, sequential VLC on normal-phase and C18-reversed-phase silica, guided at each step by both TLC profiling and in vitro α-glucosidase inhibitory activity, yielded three major active fractions from which Δ-9-tetrahydrocannabinol (**1**; THC, 76 mg; purity = 98.83%), cannabinol (**2**; CBN, 83 mg; purity =98.51%), and cannabidiol (**3**; CBD, 185 mg; purity = 99.46%) were isolated in pure form and designated as compounds 1–3, respectively. These results indicate that the strong α-glucosidase inhibitory activity of the crude cannabis extract is at least partly attributable to these three major cannabinoids. The spectroscopic and chromatographic data for the three isolated cannabinoids can be summarized as follows (**Figure 2**).

THC (1): light brown viscous oil; Rf = 0.37 (MeOH/H_2O, 95:5); UV (EtOH) λmax 278, 210 nm; IR (neat) ν_{max} 3440, 2952, 2929, 2860, 1622, 1575, 1427, 1365, 1186, 1049, 1022, 837 cm^{-1}; for ^1H NMR (500 MHz, $CDCl_3$) δ 6.33 (brt, 1H), 6.28 (d, J = 1.6 Hz, 1H), 6.15 (d, J = 1.6 Hz, 1H), 5.17 (s, 1H), 3.25-3.17 (m, 1H), 2.47-2.38 (m, 2H), 2.20-2.14 (m, 2H), 1.95-1.89 (m, 1H), 1.76-1.66 (m, 5H), 1.60-1.51 (m, 3H), 1.46-1.37 (m, 5H), 1.35-1.25 (m, 5H), 1.10 (s, 3H), 0.88 (t, J = 6.9 Hz, 3H).

CBN (2): light brown viscous oil; Rf = 0.42 (MeOH/H_2O, 95:5); UV (MeOH) λmax 280, 220 nm; IR (neat) ν_{max} 3382, 2958, 2929, 2858, 1620, 1583, 1434, 1404, 1284, 1228, 1193, 1155, 1051, 815 cm^{-1}; for ^1H NMR (500 MHz, $CDCl_3$) δ 8.28 (brs, 1H), 7.17 (d, J = 7.8 Hz, 1H), 7.11-7.07 (m, 1H), 6.47 (d, J = 1.5 Hz, 1H), 6.28 (d, J = 1.5 Hz, 1H), 5.59 (s, 1H) 2.50 (d, J = 7.6 Hz, 1H), 2.48 (d, J = 7.9 Hz, 1H), 2.41 (s, 1H), 1.66-1.57 (m, 8H), 1.40-1.30 (m, 4H), 0.92 (t, J = 6.9 Hz, 3H).

CBD (3): light yellow viscous oil; Rf = 0.55 (MeOH/H_2O, 95:5); UV

ISSN 2616-0684 (Print)
ISSN 2616-0692 (Electronic)

(MeOH) λmax 279, 209 nm; IR (neat) ν_{max} 3477, 2958, 2927, 2858, 1627, 1581, 1515, 1444, 1309, 1217, 1024, 891 cm^{-1}; for ^1H NMR (500 MHz, $CDCl_3$) δ 6.40-6.00 (m, 3H), 5.58 (brs, 1H), 4.66-4.52 (m, 2H), 3.95-3.88 (m, 1H), 2.48-2.20 (m, 3H), 2.31-2.20 (m, 1H), 2.15-2.05 (m, 1H), 1.87-1.74 (m, 5H), 1.68 (s, 3H), 1.60-1.52 (m, 2H), 1.37-1.25 (m, 4H), 0.90 (t, *J* = 7.0 Hz, 3H).

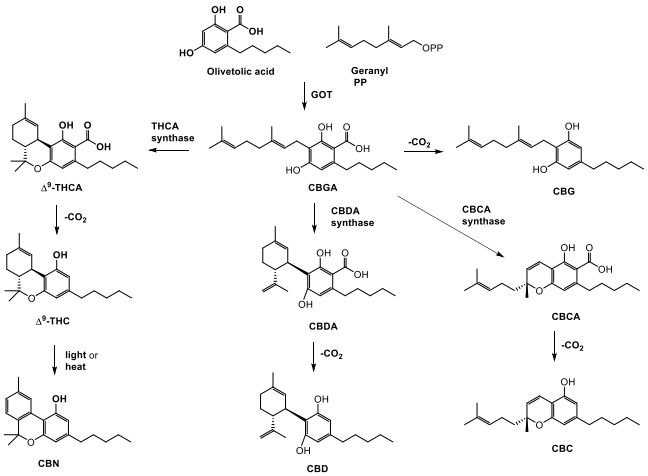

Figure 1: Biosynthetic pathway of major phytocannabinoids in Cannabis. Olivetolic acid and geranyl pyrophosphate (geranyl-PP) are condensed to form cannabigerolic acid (CBGA), the central precursor of the main cannabinoid subclasses. CBGA is converted by THCA synthase and CBDA synthase to Δ⁹-tetrahydrocannabinolic acid (Δ⁹-THCA) and cannabidiolic acid (CBDA), respectively, which undergo decarboxylation upon heating to yield Δ⁹-THC and CBD, while Δ⁹-THC can be further oxidized to cannabinol (CBN). In a parallel pathway, CBGA can be cyclized by CBCA synthase to cannabichromenic acid (CBCA), which then decarboxylates to cannabichromene (CBC), or is converted directly by heat to cannabigerol (CBG)

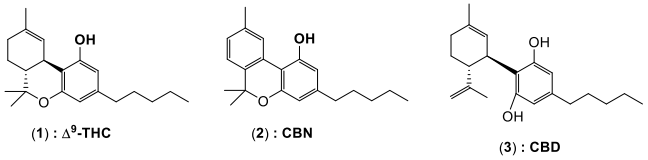

Figure 2: Chemical structures of isolated compounds from the leaves of *Cannabis sativa*. The panel shows Δ⁹-tetrahydrocannabinol (1; Δ⁹-THC), cannabinol (2; CBN), and cannabidiol (3; CBD)

Preparation of cannabis extraction

Inflorescence extracts of cannabis, following chemotypes: THC-rich (Black dragon), CBD-rich (BLC-1C), hybrid THC/CBD (CBD-purple), CBG-rich (SUT11), and CBG/CBD (1:1.3; CBG-F1). **Table 1** shows that the cannabinoid profiles of the *C. sativa* inflorescence extracts were successfully differentiated into THC-, CBD-, CBG-dominant, and hybrid chemotypes. Black Dragon exhibited a high THC content (15.85% w/w) with undetectable CBD and CBG, consistent with a THC-dominant drug-type cultivar. BLC-1C contained 8.74% w/w CBD with no detectable THC or CBG, confirming its classification as a CBD-rich chemotype. CBD-purple presented a mixed THC/CBD profile (3.53% and 2.54% w/w, respectively), whereas SUT11 accumulated predominantly CBG (3.06% w/w) in the absence of THC and CBD, representing a CBG-rich chemotype. Finally, the hybrid CBG-F1 contained both CBG (1.00% w/w) and CBD (1.33% w/w) at comparable levels, consistent with its design as a CBG/CBD-hybrid line.

Table 1: Cannabinoid profiles of the investigated *Cannabis* cultivars. Each cultivar is classified according to its chemotype and characterized by the major cannabinoids quantified in dried inflorescences

Cultivar	Chemotype	THC (%w/w)	CBD (%w/w)	CBG (%w/w)
Black Dragon	THC-dominant	15.85	-	-
BLC-1C	CBD-dominant	-	8.743	-
CBD-purple	Hybrid (THC/CBD)	3.533	2.543	-
SUT11	CBG-dominant	-	-	3.063
CBG-F1	Hybrid (CBG/CBD)	-	1.330	1.000

Together, these data demonstrate that selective breeding yielded inflorescence extracts with clearly separated major cannabinoid patterns suitable for chemotype–activity comparisons. In line with established chemotype classifications, Black Dragon fits chemotype I (THC-dominant), BLC-1C corresponds to chemotype III (CBD-dominant), and SUT11 resembles chemotype IV (CBG-dominant), whereas CBD-purple and CBG-F1 represent intermediate hybrid profiles that cannot be captured by a simple THC/CBD ratio alone. The relatively high THC content in Black Dragon is consistent with reports that drug-type inflorescences typically accumulate 3–21% THC, while fiber-type and CBD-rich plants accumulate higher proportions of CBD with low THC. The balanced CBG:CBD ratio in CBG-F1 (approximately 1:1.3) is particularly noteworthy, because this chemotype produced α-glucosidase inhibition approaching that of the THC-rich extract despite containing no major psychoactive cannabinoid, suggesting that inflorescence chemotypes enriched in non-psychoactive cannabinoids can be rationally engineered to mimic the functional potency of THC-dominant material. From a formulation perspective, the cannabinoid contents observed here fall within ranges previously reported for cannabis inflorescences, which typically contain higher levels of THC and CBD than leaves; however, the presence of CBG-dominant and CBG/CBD-hybrid profiles highlights additional diversity beyond the classical chemotype I–III framework. This diversity provides a useful platform to dissect how shifts from THC-dominant to CBD- or CBG-rich profiles—and especially to mixed CBG/CBD hybrids—translate into differences in α-glucosidase inhibition and overall antidiabetic potential. In particular, the CBG-F1 profile suggests that tuning both the identity and ratio of non-psychoactive cannabinoids in inflorescence extracts may be a viable strategy to optimize enzyme inhibition while minimizing regulatory and safety concerns associated with high-THC chemotypes. Early chemotaxonomic work defined three major chemotypes based on the THC:CBD ratio (type I: THC-dominant, type II: balanced, type III: CBD-dominant). Subsequent studies and breeding programs have expanded this to include at least two additional categories: type IV (CBG-dominant) and type V (essentially cannabinoid-free), reflecting cultivars selected for high CBG or fiber use. In parallel, the term hybrid is now used in two overlapping ways: genetically (Indica × Sativa crosses) and chemically to describe chemovars with intermediate or mixed cannabinoid profiles, such as high-THC/high-CBD hybrids or lines intentionally enriched in both major and minor cannabinoids.[16]

α-Glucosidase inhibition assay

The in vitro α-glucosidase inhibitory activities of purified cannabinoids, cannabis inflorescence extracts, and acarbose are summarized in Table 2.

ISSN 2616-0684 (Print)
ISSN 2616-0692 (Electronic)

Table 2: Inhibitory potency of purified cannabinoids and chemotyped *Cannabis* extracts against α-glucosidase

Compounds/Extracts	IC_{50} (µg/mL)
Purified compound	
THC	90.19 ± 3.14[a]
CBD	331.54 ± 7.45[b]
CBN	536.65 ± 9.85[c]
Cannabis Extracted	
Black Dragon	271.77 ± 6.98[d]
BLC-1C	952.86 ± 12.15[e]
CBD-purple	307.13 ± 3.34[f]
SUT11	456.20 ± 11.87[g]
CBG-F1	111.51 ± 8.42 [a]
Acarbose	484.10 ± 4.26 [g]

*Values with non-identical letters (a, b, c, d, e, f, and g) are significantly different ($p < 0.05$).

Among the purified compounds, THC exhibited the strongest inhibition (IC_{50} = 90.19±3.14 µg/mL), followed by CBD and CBN (331.54±7.45 and 536.65±9.85 µg/mL, respectively), establishing a clear potency rank order of THC > CBD > CBN. For crude extracts, the THC-rich Black Dragon showed the highest activity (IC_{50} = 271.77±6.98 µg/mL), whereas the CBD-rich BLC 1C was the least active (IC_{50} = 952.86±12.15 µg/mL). The CBG-rich SUT11 (456.20±11.87 µg/mL) and CBD/THC hybrid CBD purple (307.13±3.34 µg/mL) displayed moderate inhibition. Notably, the CBG/CBD hybrid CBG F1 exhibited a markedly lower IC_{50} (111.51±8.42 µg/mL), approaching the potency of purified THC despite its low total cannabinoid content (~2.33% w/w).

This highlights that inhibitory activity in crude extracts is not solely dependent on THC content but is strongly influenced by phytochemical interactions within the extract matrix.

Total phenolic content (Table 3) further supports this observation. Black Dragon and CBG F1 contained significantly higher phenolic levels (104.29±2.20 and 95.70±1.39 mg GAE/g extract, respectively). They correspondingly showed the strongest enzyme inhibition among crude extracts, whereas BLC 1C had both the lowest phenolic content and the weakest activity. Given that phenolic compounds are known α-glucosidase inhibitors, their presence likely contributes, either additively or synergistically, to enhance overall cannabinoid activity. This may partly explain the high potency of CBG F1 despite its low cannabinoid concentration.

Hybrid chemotypes provide further insight into these interactions. CBD purple showed intermediate activity, suggesting partial enhancement from combined THC and CBD. More strikingly, CBG F1, with a CBG:CBD ratio of ~1:1.3, achieved near-THC potency, indicating that specific combinations of non-psychoactive cannabinoids can produce strong inhibitory effects, potentially through synergistic mechanisms.

Overall, these findings support that α-glucosidase inhibition by cannabis extracts is governed not only by individual cannabinoids such as THC but also by the broader chemical profile, including cannabinoid ratios and co-occurring phenolics. CBG F1 emerges as a promising candidate, combining high inhibitory activity with low psychoactive risk. Further studies in cellular and in vivo systems are needed to validate its antidiabetic potential and clarify the underlying mechanisms of interaction.

The results of in vitro α-glucosidase inhibitory effects of Purified compounds, inflorescence extracts of cannabis, and acarbose are shown in **Table 2**. The purified cannabinoids showed clear differences in α-glucosidase inhibitory potency, with THC exhibiting the lowest IC_{50} value (90.19 ± 3.14 µg/mL), followed by CBD and CBN (331.54 ± 7.45 and 536.65 ± 9.85 µg/mL, respectively), indicating that THC is the most active inhibitor among the tested single compounds. These data support a potency rank order of THC > CBD > CBN at the enzyme level. For the crude chemotype extracts, the THC-rich Black Dragon sample displayed the strongest inhibition (IC_{50} = 271.77 ± 6.98 µg/mL), whereas the CBD-rich BLC-1C extract was the least active (IC_{50} = 952.86 ± 12.15 µg/mL). The CBD/THC-hybrid chemotype CBD-purple showed intermediate activity (IC_{50} = 307.13 ± 3.34 µg/mL), and the CBG-rich SUT11 extract exhibited moderate inhibition (IC_{50} = 456.20 ± 11.87 µg/mL). Notably, the CBG/CBD-rich hybrid CBG-F1 demonstrated an IC_{50} of 111.51 ± 8.42 µg/mL, which was markedly lower than those of all other crude extracts and approached the potency of purified THC itself. This finding indicates that an appropriate combination of non-psychoactive cannabinoids in CBG-F1 can yield α-glucosidase inhibition comparable to THC-rich preparations while avoiding high THC content. The present findings demonstrate that THC is the most potent α-glucosidase inhibitor among the purified cannabinoids examined, with an IC_{50} markedly lower than that of CBD and CBN, thereby confirming a clear potency rank order of THC > CBD > CBN in the enzyme assay. This pattern suggests that structural features unique to THC favor stronger interactions with the α-glucosidase active site, whereas CBD and CBN interact less efficiently and therefore display only moderate inhibitory effects. From a drug-development perspective, however, the psychoactivity and regulatory status of THC continue to limit its direct applicability as an antidiabetic ingredient despite its favorable in vitro profile. When moving from purified compounds to crude extracts, inhibition no longer correlates solely with THC content, indicating that the matrix of co-occurring phytochemicals substantially modulates overall activity. The THC-rich Black Dragon extract exhibited the strongest inhibition among the crude chemotypes, yet it remained less potent than THC alone, implying that non-cannabinoid constituents or less active cannabinoids may attenuate the effect or that THC is present at sub-optimal proportions in the extract. In contrast, CBD-rich (BLC-1C) and CBG-rich (SUT11) extracts were considerably weaker, supporting the view that dominance of a single non-psychoactive cannabinoid is insufficient to reproduce the high inhibitory potency observed for THC. Hybrid chemotypes provided further insight into possible synergistic interactions.

Table 3: Total phenolic content of Cannabis extracts

Cannabis Extracted	Total phenolic content (mg GAE/g extract)
Black Dragon	104.29±2.20[b]
BLC-1C	48.88±4.10[a]
CBD-purple	63.38±3.32[a]
SUT11	70.05±4.73[a]
CBG-F1	95.70±1.39[b]

*Values with non-identical letters (a and b) are significantly different ($p < 0.05$).

In addition to cannabinoid composition, the total phenolic content of the extracts appears to contribute to the observed α-glucosidase inhibitory activity. As shown in Table 3, Black Dragon and CBG F1 exhibited significantly higher total phenolic contents (104.29 ± 2.20 and 95.70 ± 1.39 mg GAE/g extract, respectively) compared to the other chemotypes. Notably, these two extracts also demonstrated the strongest enzyme inhibition among the crude samples, suggesting a possible correlation between phenolic content and inhibitory potency. Phenolic compounds are widely recognized for their ability to inhibit carbohydrate-hydrolyzing enzymes, including α-glucosidase, through mechanisms such as hydrogen bonding with the active site and interference with substrate binding[10]. Therefore, the relatively high phenolic content in Black Dragon and CBG F1 may act synergistically with cannabinoids to enhance overall inhibitory activity. In contrast, BLC 1C, which showed the lowest phenolic content (48.88 ± 4.10 mg GAE/g extract), also exhibited the weakest α-glucosidase inhibition,

ISSN 2616-0684 (Print)
ISSN 2616-0692 (Electronic)

further supporting this relationship. Importantly, the exceptional potency of CBG F1, despite its relatively low total cannabinoid content (~2.33% w/w), may be partially explained by the combined effects of its cannabinoid profile and its enriched phenolic matrix. This finding highlights that enzyme inhibition in cannabis extracts is not solely dependent on major cannabinoids but is also significantly influenced by co-occurring phenolic constituents and their interactions within the extract matrix.

The CBD/THC-hybrid CBD-purple showed intermediate activity, with an IC_{50} lower than that of the CBD- and CBG-dominant extracts but higher than that of the THC-rich Black Dragon, suggesting that moderate amounts of THC combined with CBD can partially enhance α-glucosidase inhibition without reaching the potency of a fully THC-rich profile. Most strikingly, the CBG/CBD-rich hybrid CBG-F1 achieved an IC_{50} close to that of purified THC and substantially lower than all other crude extracts, including Black Dragon. This result implies that specific combinations of non-psychoactive cannabinoids—here, a CBG:CBD ratio of approximately 1:1.3—can yield a functional potency that rivals THC-rich preparations, possibly through synergistic or additive effects at the enzyme level. Taken together, these observations support a model in which α-glucosidase inhibition by cannabis-derived preparations is determined not only by the presence of highly active single molecules such as THC but also by the broader cannabinoid profile and intramatrix interactions. CBG-F1 emerges as a particularly attractive candidate because it reconciles high inhibitory potency with the absence of high THC levels, thereby reducing concerns regarding psychoactivity and regulatory control while retaining strong functional activity against α-glucosidase. Further work using cellular and in vivo models will be required to confirm whether the in vitro advantages of CBG-F1 translate into superior glycemic control and to elucidate the molecular basis of the apparent synergy between CBG and CBD.

The co-occurrence of THC, CBD, CBN, and CBG in hybrid chemovars broadens the range of biological activities beyond those predicted by the THC:CBD ratio alone. THC-rich or THC-hybrid chemovars drive classical CB1-mediated psychoactive and analgesic actions, but, through THC oxidation, also generate CBN, which contributes additional sedative, analgesic, and—in α-glucosidase assays—often comparatively strong inhibitory activity. CBD-rich and CBD-hybrid chemovars contribute non-psychoactive anti-inflammatory and antiepileptic effects, and together with oxidized CBD-type metabolites and phenolic co-constituents, provide meaningful α-glucosidase inhibition that can rival or exceed single-compound effects.[10] CBG-dominant or CBG-enriched hybrids add further dimensions. While CBG has not consistently emerged as the most potent isolated α-glucosidase inhibitor, CBG-rich profiles are associated with anti-inflammatory and analgesic actions and may modulate metabolic pathways that complement direct enzyme inhibition by THC/CBN-type compounds. At the same time, hybrid chemovars selected for high CBG alongside moderate THC and CBD exemplify how breeding can intentionally combine multiple mechanisms—central analgesia, peripheral anti-inflammation, and α-glucosidase inhibition—within a single chemovar. Consequently, when evaluating α-glucosidase inhibition and broader bioactivity, it is increasingly important to consider not only THC and CBD chemotypes but also the hybrid context and the embedded profiles of CBN, CBG, and other minor cannabinoids, which jointly shape the therapeutic potential of contemporary *C. sativa* varieties.[10]

Kinetic Study of α-Glucosidase Inhibition

Regarding the enzyme kinetic studies shown in **Figure 3**, the Lineweaver–Burk plots clearly indicated that the CBG-F1 extracted exhibits a non-competitive inhibition mode against the yeast alpha-glucosidase. These results demonstrate that inhibition occurs through binding of the compound to an allosteric site rather than the active site where the substrate typically binds. This mechanism is distinct from that of competitive inhibitors such as acarbose, which compete directly at the active site.

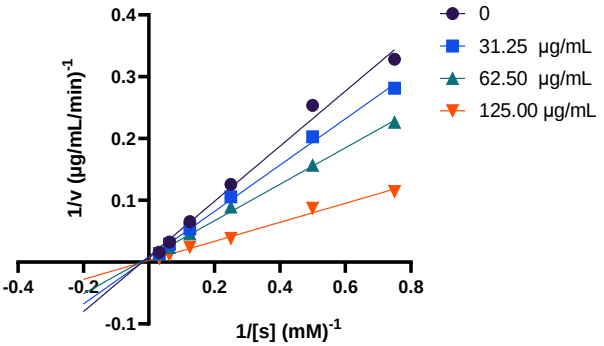

Figure 3: Lineweaver–Burk plots showing the effect of the CBG-rich cannabis extract; CBG-F1 on yeast α-glucosidase activity at various inhibitor concentrations (0, 31.25, 62.50 and 125.00 µg/mL). The reciprocal plots of 1/v versus 1/[S] display a family of straight lines that intersect on the x-axis while exhibiting progressive decreases in the y-intercept (1/Vmax*Vmax*) with increasing inhibitor concentration, indicating a non-competitive mode of inhibition.

In this non-competitive model, the inhibitor binds with equal affinity to both the free enzyme (E) and the enzyme-substrate complex (ES). Consequently, the maximum reaction velocity (Vmax) decreases as the concentration of the inhibitor increases, while the Michaelis constant (Km) remains constant, signifying that the substrate binding affinity is not affected by the presence of the inhibitor. (**Figure 4**) To further quantify the inhibitory potency, the inhibition constant (Ki) was determined. By analyzing the secondary plots derived from the Lineweaver–Burk data, the Ki value was calculated to be 92.82 µg/mL. This Ki value represents the dissociation constant of the enzyme-inhibitor complex, while a lower value would indicate stronger binding affinity. The identification of this non-competitive behavior is consistent with compounds that possess significantly different chemical structures from the natural substrate, preventing them from fitting into the catalytic pocket but allowing them to modulate enzyme activity from a distant site.

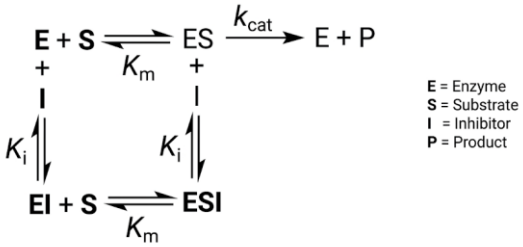

Figure 4: Kinetic scheme of non-competitive inhibition. The inhibitor (I) binds with equal affinity to both the free enzyme (E) and the enzyme-substrate complex (ES), characterized by the inhibition constant (Ki). In this model, the formation of the inactive ESI complex reduces the effective concentration of the active enzyme, thereby decreasing the maximum reaction velocity (Vmax) while keeping the Michaelis constant (Km) constant.

In this study, the Lineweaver–Burk analysis demonstrated that the CBG-F1 fraction inhibits yeast α-glucosidase via a non-competitive, allosteric mechanism, lowering Vmax without altering Km, which indicates that substrate binding remains intact while catalytic turnover is attenuated even at high substrate concentrations; this mechanistic profile contrasts with the classical competitive inhibitor acarbose,

which directly competes with substrates at the active site and therefore loses relative effectiveness as substrate levels rise, and it aligns with recent reports that non-competitive, allosteric plant-derived and cannabinoid-based α-glucosidase inhibitors can offer more robust postprandial glucose control and may help overcome some efficacy and tolerability limitations associated with existing competitive drugs such as acarbose, miglitol, and voglibose.[4]

Conclusion

In conclusion, this study demonstrates that cannabinoids from *Cannabis* sp. possess significant potential as alpha-glucosidase inhibitors, with a rank order of potency of THC > CBD > CBN for purified compounds. While THC-rich extracts exhibited strong inhibitory activity, their psychoactive properties and regulatory restrictions limit their therapeutic application. Notably, the CBG/CBD-rich hybrid chemotype (CBG-F1), characterized by a CBG to CBD ratio of approximately 1:1.3, emerged as the most promising non-psychoactive candidate. CBG-F1 achieved an IC_{50} value of 111.51 ± 8.42 µg/mL, which is comparable to the potency of purified THC and superior to other tested crude extracts. Enzyme kinetic analysis using Lineweaver–Burk plots further revealed that CBG-F1 operates via a non-competitive inhibition mechanism with an inhibition constant (Ki) of 92.82 µg/mL. This indicates that the bioactive constituents in CBG-F1 bind to an allosteric site rather than the active site, effectively reducing the catalytic rate (Vmax) without altering the substrate binding affinity (Km). These findings suggest that the specific combination of non-psychoactive cannabinoids in CBG-F1 may exert synergistic or additive effects, providing a functional potency that rivals THC-dominant preparations. Consequently, CBG-F1 represents a safe, non-psychoactive, and highly effective functional ingredient for the development of supportive antidiabetic nutraceuticals and pharmaceutical products.

Conflict of Interest

The authors declare no conflict of interest.

Authors' Declaration

The authors hereby declare that the work presented in this article is original and that any liability for claims relating to the content of this article will be borne by them.

Acknowledgements

This research was supported by Thaksin University (Grant No. TSU67-INV002) and under the Technology to Industry Convergence Program (P4), Southern Science Park, in collaboration with industrial partners. The authors would like to thank the Faculty of Science and Digital Innovation, Thaksin University, and the Faculty of Science and Technology, Phuket Rajabhat University, for providing laboratory facilities and research infrastructure.The authors also gratefully acknowledge Kannabiz Tech Co., Ltd. for their valuable industrial collaboration, particularly for their technical support and expertise in HPLC analysis, which significantly contributed to the reliability and successful completion of this study.

References

1. Fordjour E, Manful CF, Sey AA, Javed R, Pham TH, Thomas R, Cheema M. Cannabis: a multifaceted plant with endless potentials. Front Pharmacol. 2023;14:1200269.doi: 10.3389/fphar.2023.1200269
2. Duczmal D, Bazan-Wozniak A, Niedzielska K, Pietrzak R. Cannabinoids-Multifunctional Compounds, Applications and Challenges-Mini Review. Molecules. 2024;29(20).4923. doi:10.3390/molecules29204923
3. Avoseh FT, Mtunzi FM, Avoseh ON, Takaidza S. *Cannabis sativa*; Ethnobotanicals, Classifications, Pharmacology, and Phytochemistry. Nat Prod Commun. 2025;20(6). doi:10.1177/1934578X251334244
4. Dirir AM, Daou M, Yousef AF, Yousef LF. A review of alpha-glucosidase inhibitors from plants as potential candidates for the treatment of type-2 diabetes. Phytochem Rev. 2022;21(4):1049-1079. doi: 10.1007/s11101-021-09773-1
5. Hossain U, Das AK, Ghosh S, Sil PC. An overview on the role of bioactive α-glucosidase inhibitors in ameliorating diabetic complications. Food Chem Toxicol. 2020;145:111738. doi: 10.1016/j.fct.2020.111738
6. Şöhretoğlu D, Renda G, Arroo R, Xiao J, Sari S. Advances in the natural α-glucosidase inhibitors. eFood. 2023;4(5):e112. doi: 10.1002/efd2.112
7. Suttithumsatid W, Shah MA, Bibi S, Panichayupakaranant P. α-Glucosidase inhibitory activity of cannabidiol, tetrahydrocannabinol and standardized cannabinoid extracts from *Cannabis sativa*. Curr Res Food Sci. 2022;5:1091-1097. doi:10.1016/j.crfs.2022.07.002
8. Bridgeman MB, Abazia DT. Medicinal Cannabis: History, Pharmacology, And Implications for the Acute Care Setting. PT. 2017;42(3):180-188.
9. Casajuana Köguel C, López-Pelayo H, Balcells-Olivero MM, Colom J, Gual A. Psychoactive constituents of cannabis and their clinical implications: a systematic review. Adicciones. 2018;30(2):140-151. doi: 10.20882/adicciones.858
10. Nguyen A-K, Lerttanakij P, Taweechat P, Sompornpisut P, Khotwong S, Wacharasindhu S, Phuwapraisirisan P. α-Glucosidase Inhibitors from the Leaves of *Cannabis sativa*: Structure–Activity Relationship, Kinetic Investigation, and Molecular Docking. J Agric Food Chem. 2025;73(33):20900-20915. doi: 10.1021/acs.jafc.5c08443
11. Krzyżewska A, Kloza M, Kozłowska H. Comprehensive mini-review: therapeutic potential of cannabigerol - focus on the cardiovascular system. Front Pharmacol. 2025;16:1561385. doi: 10.3389/fphar.2025.1561385
12. Ma H, Li H, Liu C, Seeram NP. Evaluation of cannabidiol's inhibitory effect on alpha-glucosidase and its stability in simulated gastric and intestinal fluids. J Cannabis Res. 2021;3(1):20. doi: 10.1186/s42238-021-00077-x
13. Gallily R, Zhanna Y, Hanus L. Overcoming the Bell-Shaped Dose-Response of Cannabidiol by Using Cannabis Extract Enriched in Cannabidiol. Pharmacol Pharm 2015;06:75-85. doi:10.4236/PP.2015.62010
14. Ferber SG, Namdar D, Hen-Shoval D, Eger G, Koltai H, Shoval G, Shbiro L, Weller A. The "Entourage Effect": Terpenes Coupled with Cannabinoids for the Treatment of Mood Disorders and Anxiety Disorders. Curr Neuropharmacol. 2020;18(2):87-96.doi: 10.2174/1570159X17666190903103923
15. Blasco-Benito S, Seijo-Vila M, Caro-Villalobos M, Tundidor I, Andradas C, García-Taboada E, Wade J, Smith S, Guzmán M, Pérez-Gómez E, Gordon M, Sánchez C. Appraising the "entourage effect": Antitumor action of a pure cannabinoid versus a botanical drug preparation in preclinical models of breast cancer. Biochem Pharmacol. 2018;157:285-293. doi: 10.1016/j.bcp.2018.06.025.
16. Langa S, Magwaza LS, Mditshwa A, Tesfay SZ. Characterization of cannabis varieties and the intrinsic and extrinsic factors affecting cannabis germination and seedling establishment: A descriptive review. Industrial Crops and Products. 2024;208:117861. doi: 10.1016/j.indcrop.2023.117861